Plate kinematics in the western Pacific derived from geodetic observations

Paul Tregoning
Research School of Earth Sciences, Australian National University, Canberra, A.C.T., Australia

Received 1 May 2000; revised 13 November 2000; accepted 22 August 2001; published 29 January 2002.

[1] Plate kinematics have been derived from GPS site velocities spanning Australasia and the western Pacific and define a framework in which deformation fields at plate boundaries can be investigated. The Australian Plate appears to be rigid from Cocos Island in the west to Noumea in the east and incorporating all of the Australian continent. A revision of the angular velocity vector of the Pacific Plate using six site velocities has led to the detection of significant relative motion between the Pacific Plate and sites in northern Papua New Guinea. This provides strong evidence in support of a North Bismarck Plate between the South Bismarck and Pacific Plates and we model the motion of the North Bismarck Plate with the angular velocity vector (45.0°S, 126.4°E, 0.85°/Myr). These new angular velocity vectors model the rigid plate motions of a substantial part of the Australasian and western Pacific regions with an accuracy better than 3 mm/yr. *INDEX TERMS:* 1206 Geodesy and Gravity: Crustal movements–interplate (8155), 1243 Geodesy and Gravity: Space geodetic surveys, 8158 Tectonophysics: Plate motions–present and recent (3040), 3040 Marine Geology and Geophysics: Plate tectonics (8150, 8155, 8157, 8158); *KEYWORDS:* GPS, North Bismarck Plate, Australian Plate, Pacific Plate, tectonic motion

1. Introduction

[2] Southeast Asia and the western Pacific are tectonically complex and active regions which, encompassing the collisions of the Australian, Pacific, and Eurasian Plates, include several microplates such as the South Bismarck Plate (Figure 1). Several authors [e.g., *Seno et al.*, 1993; *Kato et al.*, 1996; *Tregoning et al.*, 1998a] have presented models of the motion of some of these plates in the region derived using combinations of geologic, seismic, and geodetic data.

[3] The focus of this paper is to define accurate angular velocity vectors which model the rigid motion of these plates. Such models can then be used to remove the rigid plate motion component from local monitoring networks spanning plate boundaries in order to derive relative deformation patterns at the margins. We use recent geodetic data spanning the Australian Plate and the western Pacific region to derive new tectonic models of the motions of the Australian and Pacific Plates. We also provide the first estimate of the motion of the North Bismarck Plate. Since the above mentioned plates interact at over 15 distinct subduction zones, spreading centers, and strike-slip boundaries, we use the modeled motions to predict the relative motion across only some specific plate boundaries.

2. Tectonic Setting and Existing Models

[4] The Australian and Pacific Plates collide across a very long margin, stretching from southern New Zealand through the South Pacific, the New Hebrides subduction zone, and farther north to the San Cristobal Trench in the Solomon Islands (Figure 1). The South Bismarck Plate is trapped between the Australian and Pacific Plates in Papua New Guinea and is rotating clockwise at ∼8°/Myr in response to this collision [*Tregoning et al.*, 1999].

[5] *Johnson and Molnar* [1972] proposed the existence of a North Bismarck Plate, located between the South Bismarck and Pacific Plates, on the basis of an E-W belt of seismicity at 4°S and by a minor belt of activity in the northern part of the Bismarck Sea. They considered the northern boundary of the North Bismarck Plate to be the Manus Trench running from the New Guinea coastline eastwards to join with the Kilinailau Trench east of New Ireland. Other authors have questioned the existence of a North Bismarck Plate [e.g., *Curtis*, 1973; *Krause*, 1973; *Taylor*, 1979]. *Tregoning et al.* [1998a] presented the velocities of two sites in northern Papua New Guinea whose motion, to a first-order approximation, appeared to be consistent with the Pacific Plate motion, although they did note an apparent coherence of the deviation from predicted Pacific Plate motion at both sites. These two sites, Kavieng (KAVI) and Manus Island (MANU), are located north of the Bismarck Sea Seismic Lineation and would be located on a North Bismarck Plate if it were to exist. *Tregoning et al.* [1998a] concluded that any possible deviations from Pacific Plate motion at these sites were within the uncertainties of their velocity estimates.

[6] The motion of the South Bismarck Plate was modeled by *Tregoning et al.* [1999] from four GPS velocities. This plate comprises the Southern Bismarck Sea, New Britain, and the Huon Peninsula and stretches at least as far west as Madang. *Weiler and Coe* [2000] confirmed from palaeomagnetic studies that the Huon Peninsula appears to be undergoing a rigid rotation and that there were no apparent relative motions between blocks in the Finisterre Range. In the geodetic analysis presented below, we used the same geodetic data as used by *Tregoning et al.* [1999] to estimate an angular velocity vector for the South Bismarck Plate. Our estimate is not significantly different from their earlier result, with changes in predicted motion being generally <2 mm/yr, and in this paper we used their definition of the motion of this plate.

[7] The Philippine Sea Plate is bounded on all sides by subduction zones [*Seno et al.*, 1993]. Motion of this plate has been estimated from slip vector azimuths and the best fitting pole derived from plate closures of the Eurasian, Pacific, and Caroline Plates [*Seno et al.*, 1993]. Some geodetic information was used in revised estimates of the plate motion relative to the Eurasian Plate [*Kato et al.*, 1996; *Kotake et al.*, 1998]. GPS data observed at sites on the Philippine Sea Plate are not freely available; therefore we

0148-0227/02/2001JB000406$09.00

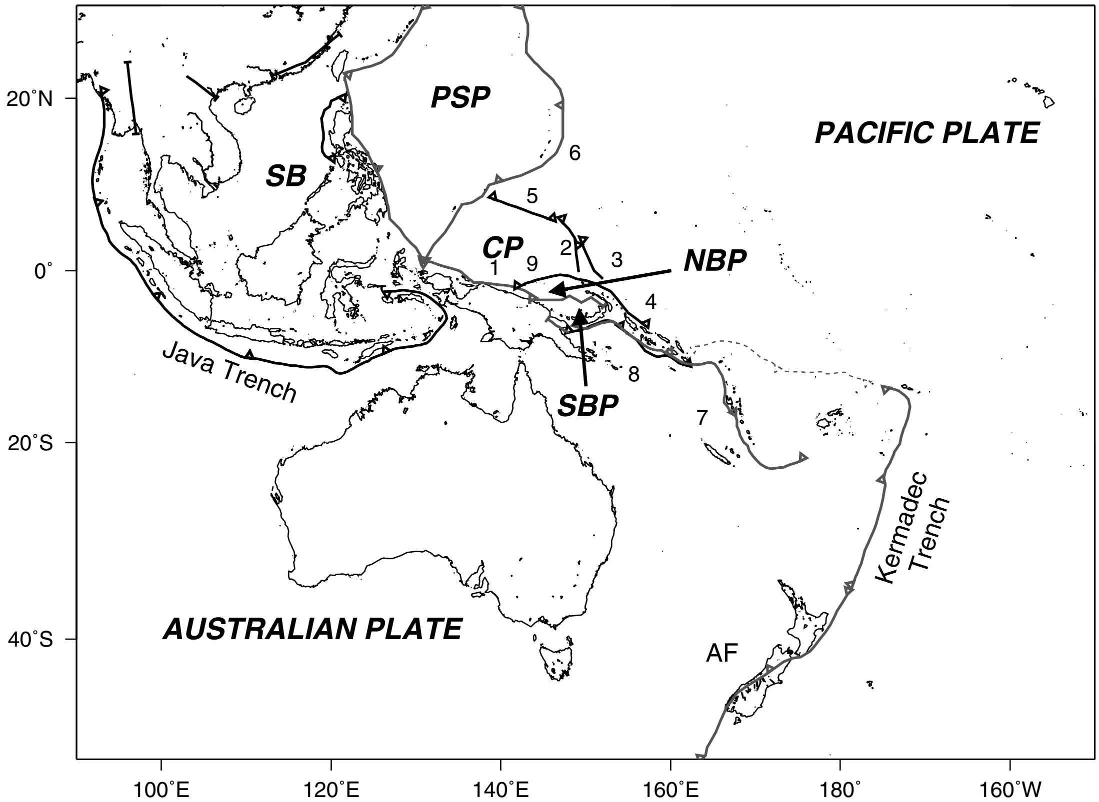

Figure 1. Major tectonic features in the study area. PSP, Philippine Sea Plate; CP, Caroline Plate; NBP, North Bismarck Plate; SBP, South Bismarck Plate; AF, Alpine Fault; 1, New Guinea Trench; 2, Mussau Trench; 3, Lyra Trough; 4, Kilinailau Trench; 5, Sorol Trough; 6, Mariana Trench; 7, Philippine Trench; 8, Manila Trench; 9, Red River Fault; 10, New Hebrides Subduction Zone; 11, San Cristobal Trench; 12, Manus Trench.

are not able to reestimate the motion of this plate as part of this analysis.

[8] *Weissel and Anderson* [1978] suggested that an additional plate, the Caroline Plate, separated the Pacific Plate from the Philippine Sea Plate farther west. They defined the boundaries of the Caroline Plate as the Manus and New Guinea Trenches in the south, the Mussau Trench in the east, and the Sorol Trough to the north, with the western boundaries with the Philippine Sea Plate being the Ayu Trough and the Palau and Yap Trenches. There is no land on the region assigned to be the Caroline Plate; therefore it is not possible to observe geodetically the motion of this plate. Redefining the motion of the Caroline Plate will be the subject of future work, and we do not consider it further in this paper.

[9] Table 1 lists some of the previous estimates of angular velocity vectors which model the motions of these plates. Using more recent data, we revise these models to estimate improved angular velocity vectors for three of the plates mentioned above.

3. Geodetic Data

[10] The geodetic data used in this analysis have been collected primarily from global tracking stations of the International GPS Service (IGS) and from campaign-style GPS surveys in Papua New Guinea [*McClusky et al.*, 1994; *Tregoning et al.*, 1998a, 1999, 2000] and Indonesia [*Tregoning et al.*, 1994], along with observations made at Wuvulu in November 1999 and Manus in October 2000.

[11] The data were analyzed as daily global solutions using the GAMIT/GLOBK software [*King and Bock*, 1999; *Herring*, 1999] to combine regional data with data from up to 80 IGS stations. We solved for a free network global polyhedron which we then aligned with the ITRF97 [*Boucher et al.*, 1999] by computing Helmert transformations on the coordinates and velocities of the 47 class A and B core IGS sites [*Altamimi*, 1998]. These analysis procedures have been well documented by, for example, *Feigl et al.* [1993], *Dong et al.* [1998], and *Tregoning et al.* [1998a]. Detailed information regarding the geodetic solution presented in this paper is provided in Appendix A. Site velocities (referenced to ITRF97) are shown in Figure 2 and are listed in Table 2.

[12] From an analysis of noise characteristics of GPS sites in southern California, *Johnson and Agnew* [2000] showed that the time series of estimates of GPS positions do not display the characteristics of white noise; rather, they resemble a random walk with a stochastic variation of at least 0.33 mm^2/yr. They suggested that this might represent instability of attaching the antennae to the ground marks, although there may be other causes for these characteristics (such as mismodeled satellite orbits and reference frame errors [*Mao et al.*, 1999]). While we do not have continuous data at most of the sites in our analysis, we included a random walk component with an amplitude of 0.33 mm^2/yr at each site to model the random walk nature of the noise. This increases the uncertainties of the velocity estimates by a factor of $\sim$2; we believe that this is a realistic increase and leads to a better estimate of the true uncertainties of the velocity estimates.

4. Angular Velocity Vector Estimation

4.1. Australian Plate

[13] We used the velocities of 10 sites located on the Australian Plate to estimate the angular velocity vector which represents the motion of the rigid plate (Figure 2). The sites comprise IGS sites at Yarragadee (YAR1), Tidbinbilla (TIDB), Hobart (HOB2), Auckland (AUCK), Cocos Islands (COCO), Perth (PERT), and Noumea (NOUM), while the remaining sites (Alice Springs (ALIC), Karra-

Table 1. Absolute and Relative Angular Velocity Vectors for the Australian, Pacific North Bismarck, and South Bismarck Plates[a]

	Latitude	Longitude	Rate, deg/Myr	Pole Error Ellipse		
				σ_{maj}	σ_{min}	Azimuth
Angular Velocity Vectors						
Australian Plate						
This study	35.1	36.5	0.619±0.004	0.8	0.3	287
ITRF97	34.3	38.5	0.608±0.004	0.9	0.2	300
NNR-1A[b]	33.8	33.2	0.65	–	–	–
Tregoning et al. [1998a][c]	31.6	41.3	0.62±0.01	2.89	1.36	293
Pacific Plate						
This study	−64.3	114.2	0.649±0.005	1.6	0.4	82
ITRF97	−64.2	116.9	0.644±0.004	1.8	0.3	84
NNR-1A	−63.0	107.4	0.64	–	–	–
DeMets and Dixon [1999]	−64.5	110.6	0.665±0.010	2.3	1.0	83
Tregoning et al. [1998a]	−61.4	105.0	0.63±0.01	2.80	1.13	54
North Bismarck Plate						
This study	−45.0	126.4	0.85±0.07	5.5	0.5	36
South Bismarck Plate						
Tregoning et al. [1999]	6.75	−32.02	8.11±0.16	0.10	0.06	4
Relative Angular Velocity Vectors						
Australian/Pacific						
This Study	−60.9	184.9	1.077±0.008	0.8	0.5	262
Tregoning et al. [1998a]	−61.4	186.8	1.01±0.02	2.38	2.28	84
Larson et al. [1997]	−65.7	182.9	1.04±0.02	1.7	1.5	2
Argus and Heflin [1995]	−57.2	186.5	1.13±0.04	2.6	2.4	43
Other plate pairs (this study)						
North Bismarck/Australian	50.6	−13.3	1.23±0.07	4.1	0.4	37
North Bismarck/Pacific	2.7	−43.2	0.3±0.1	3.5	1.4	95
North Bismarck/South Bismarck	10.2	−33.5	8.75±0.2	0.2	0.1	7

[a] Some previous estimates of the motions of some of these plates are listed for comparison. Rotation is in a clockwise direction about the pole. The error ellipses of the poles are described by the 1σ semimajor and semiminor axes of each error ellipse and the clockwise angle from true north of the semimajor axis.
[b] No-net-rotation-Nuvel-1A (NNR-1A) model [*DeMets et al.*, 1990; *Argus and Gordon*, 1991; *DeMets et al.*, 1994].
[c] Angular velocity vectors were estimated in the ITRF94 reference frame.

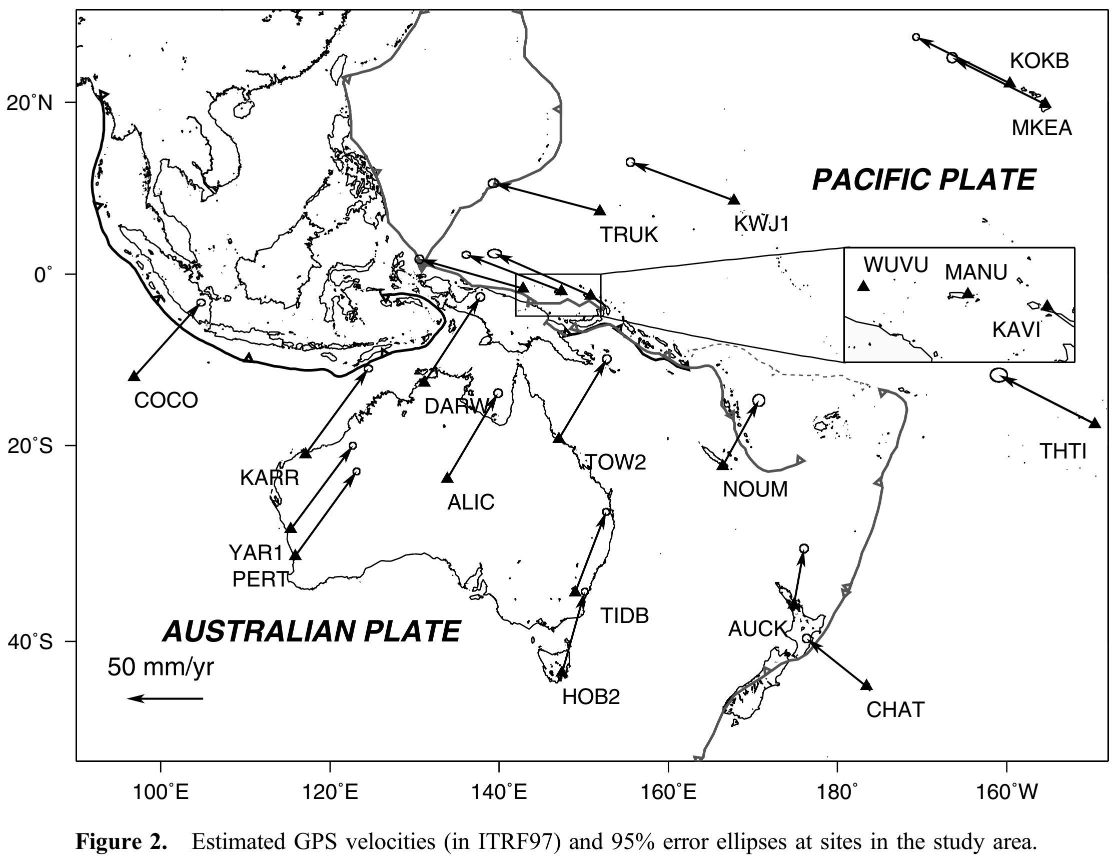

Figure 2. Estimated GPS velocities (in ITRF97) and 95% error ellipses at sites in the study area.

Table 2. Site Codes, Observed Absolute Site Velocities and Associated (1σ) Uncertainties[a]

Site	Latitude	Longitude	Data Span	ITRF97 Velocity				Model	
				V_n	V_e	σ_{V_n}	σ_{V_e}	V_n	V_e
				Australian Plate					
ALIC	23°40.1′S	133°53.2′E	95.0–00.8	55.7	33.0	1.1	1.1	−0.1	−0.4
AUCK	36°36.0′S	174°49.5′E	95.7–00.8	36.8	6.6	1.0	1.1	−0.6	−0.3
COCO	12°11.2′S	96°49.5′E	92.6–00.4	48.6	43.6	0.9	1.1	−0.3	−1.0
DARW	12°50.2′S	131°07.5′E	93.7–00.8	56.0	36.6	1.1	1.1	−0.1	−1.1
HOB2	42°48.0′S	147°26.2′E	94.7–00.8	53.0	14.8	1.0	0.9	0.5	−0.8
KARR	20°58.5′S	117°06.0′E	93.6–00.8	55.9	41.0	0.9	1.1	0.4	0.7
NOUM	22°16.1′S	166°24.4′E	98.0–00.8	42.7	23.6	1.5	1.6	−0.5	0.5
PERT	31°48.0′S	115°53.2′E	93.6–00.8	55.2	40.0	0.9	0.9	−0.1	0.8
TIDB	35°24.0′S	148°58.4′E	92.6–00.5	52.5	20.0	0.8	0.9	0.5	0.0
TOW2	19°16.1′S	147°03.4′E	95.4–00.8	52.1	31.1	1.1	1.1	−0.6	0.2
YAR1	29°03.0′S	115°21.0′E	91.1–00.8	54.5	40.5	0.8	0.9	−0.7	0.5
				Pacific Plate					
CHAT	43°57.4′S	176°34.1′E	95.8–00.8	31.1	−39.1	1.0	1.1	2.0	0.1
KOKB	22°07.5′N	159°39.4′W	91.1–00.8	30.2	−61.0	0.9	0.9	−1.0	0.2
KWJ1	08°43.1′N	167°43.5′E	96.2–00.8	25.1	−67.4	1.1	1.4	−0.1	−0.2
MKEA	19°48.0′N	155°27.4′W	96.8–00.8	30.3	−60.6	1.3	1.3	−1.0	−0.7
THTI	17°34.6′S	149°36.4′W	98.4–00.8	32.0	−62.4	1.8	2.3	0.9	0.7
TRUK	07°27.0′N	151°53.2′E	94.3–99.7	18.3	−69.3	1.1	1.3	−0.7	−1.6
				North Bismarck					
KAVI	02°34.5′S	150°48.4′E	92.4–98.7	27.4	−62.5	1.1	1.7	−0.1	1.6
MANU	02°03.0′S	147°21.6′E	93.7–00.8	23.8	−62.0	0.9	1.2	−0.1	2.6
WUVU	01°43.8′S	142°50.2′E	93.7–99.9	19.1	−67.6	1.1	1.1	0.2	−2.6

[a] Sites are listed under the plate on which they reside and velocities with respect to our model for this plate are also listed. Units are mm/yr.

tha (KARR), and Townsville (TOW2)) are part of the Australian Regional Geodetic Network [*Manning et al.*, 1998]. All data are freely available at IGS data centers. The data span for each site is typically ~4–5 years, although longer for some sites (e.g., YAR1, TIDB) (Table 2).

[14] Figure 3 shows the residual velocities at these sites after removing our predicted motion of the Australian Plate (Table 1). The motion of all of these sites can be modeled to within ~1 mm/yr by a rotation about a single Euler pole. This confirms that the whole expanse of the Australian Plate from ~96°E to the New Hebrides subduction zone in the South Pacific is moving as a rigid entity. The estimated motion of the Australian Plate using the published ITRF97 velocities at TIDB, YAR1, COCO, PERT, and AUCK is essentially the same as our estimate presented here (see Table 1).

4.2. Pacific Plate

[15] We estimated the angular velocity vector for the Pacific Plate from the velocities of five IGS sites (Chatham Island (CHAT), Manau Kea (MKEA), Kokee Park (KOKB), Kwajelein (KWJ1), Tahiti (THTI)) and one site from the Western Pacific Integrated Network of GPS (WING) [*Kato et al.*, 1998] (Truk Lagoon (TRUK)) (Figure 4). Site velocities can be modeled to within ~1.5 mm/yr by the rotation about a single Euler pole.

[16] There have been several estimates of the angular velocity vector for the Pacific Plate based on GPS site velocities. *Larson et al.* [1997] estimated an angular velocity vector in ITRF94 [*Boucher et al.*, 1996], using only two sites on the Pacific Plate. The estimate of *Tregoning et al.* [1998a] in ITRF94 used seven sites and differed considerably from that of *Larson et al.* [1997]. *DeMets and Dixon* [1999] used data from five IGS sites to estimate

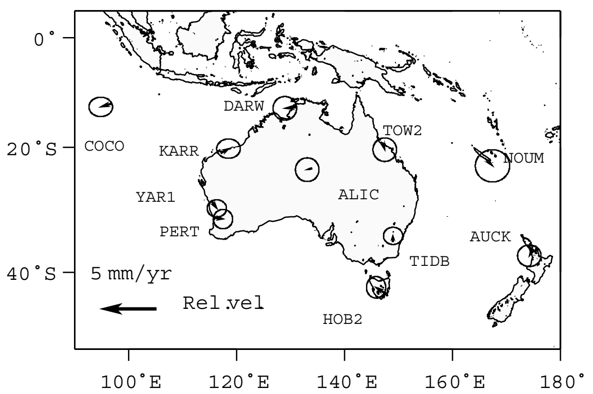

Figure 3. Velocities of sites on the Australian Plate relative to our predicted motion of the Australian Plate. The 66% error ellipses are plotted. Some of the relative vectors are so small that they are barely visible.

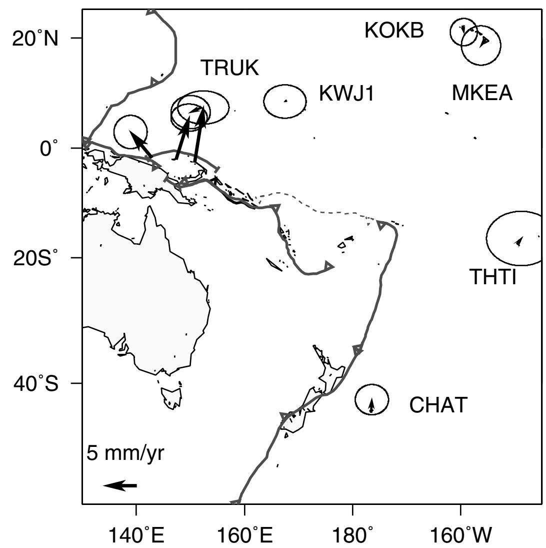

Figure 4. Velocities of sites on the Pacific Plate relative to our predicted motion of the Pacific Plate. The 95% error ellipses are plotted. The relative motions of sites in northern Papua New Guinea with respect to the Pacific Plate are clearly apparent.

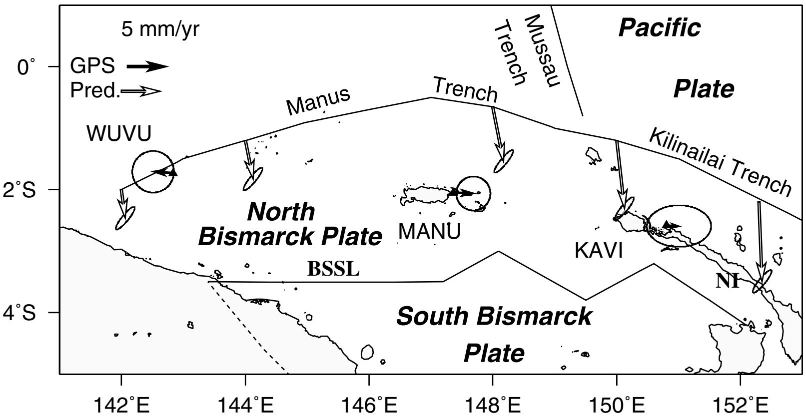

Figure 5. GPS Velocities (solid arrows) of sites on the North Bismarck Plate relative to our predicted motion of this plate. Predicted motions of the Pacific Plate relative to the North Bismarck Plate (open arrows) are plotted. The 95% error ellipses are plotted on the GPS velocities. BSSL, Bismarck Sea Seismic Lineation; NI, New Ireland.

the vector in ITRF96 [*Sillard et al.*, 1998] (Table 1) and derived a value similar to this study. The estimates from different investigators are converging on similar values as the time span of the geodetic data increases and the distribution of sites spanning the Pacific Plate improves. The estimated angular velocity vector using the published ITRF97 velocities of sites on the Pacific Plate agrees closely with our estimate (Table 1).

4.3. North Bismarck Plate

[17] *Tregoning et al.* [1998a] estimated the velocities of MANU and KAVI from GPS data observed between 1990 and 1996. Using additional data observed since 1996, we have reestimated the velocities at these two sites along with the velocity of a third site, Wuvulu (WUVU) located north of the Bismarck Sea Seismic Lineation.

[18] The relative motion of each site with respect to the Pacific Plate is significantly different at the 95% confidence level (Figure 4), partly because of improvements in the site velocity estimates and partly because of changes in the predicted motion of the Pacific Plate. For example, the difference in predicted motion at KAVI using our angular velocity vector for the Pacific Plate and that of, say *Tregoning et al.* [1998a] is +6.1 mm/yr in north and +4.6 mm/yr in east. Our estimated velocities (and associated uncertainties) differ to those of *Tregoning et al.* [1998a] because of significantly longer data records on global tracking sites, additional data observed at KAVI (in 1998) and MANU (in 2000), and the use of a more accurate terrestrial reference frame.

[19] In order to model the motion of a plate one must assume that the plate is a rigid entity, implying that there will be no change in baseline lengths between sites located on the plate. In the case of the Australian and Pacific Plates above, this assumption is valid with no rate of change of baseline lengths being statistically significantly different from zero at the 95% confidence level (typically <2 mm/yr). This may not be the case for the three sites discussed here with WUVU possibly moving relative to MANU and KAVI at ∼4–5 mm/yr. The site at WUVU has been observed only in 1993 and 1999; hence we have no redundancy in the estimate of the site velocity. Of course, these three sites may not lie on the same rigid body.

[20] Lacking any further information, we used the velocities of KAVI, MANU, and WUVU to estimate an angular velocity vector for the North Bismarck Plate (Table 1). The three site velocities can be modelled to within ∼3 mm/yr (∼95% confidence level) about a single Euler pole (Figure 5) which is a considerably better fit to the observed velocities than modelling the sites as part of the Pacific Plate (Figure 3). This provides strong support for the existence of a North Bismarck Plate, and we include this plate in our kinematic model of the region.

5. Discussion

5.1. Pacific/Australian Boundary

[21] The Pacific and Australian Plates collide along a very long boundary in the southwestern Pacific. Here we look only at the Alpine Fault, New Zealand, where relative motion between the two plates has been estimated from a dense GPS network spanning the Alpine Fault.

[22] *Beavan et al.* [1999] deduced estimates of fault-parallel and fault-normal convergence by deriving numerical fault models to fit a velocity field of over 100 GPS sites spanning the Alpine Fault. They concluded that the predicted fault-parallel relative motion from their various models were not significantly different from the model of *Tregoning et al.* [1998a] (38.8 ± 1.8 mm/yr fault-parallel, 7.5 ± 0.6 mm/yr fault-normal) but indicated that the observed fault-normal convergence (10 ± 1.6 mm/yr) was higher than predicted. They suggested that predicted motion using the model of *Tregoning et al.* [1998a] may not be sufficiently oblique to match the observed velocities and showed that the predicted relative motion using earlier models (e.g., those of *Larson et al.* [1997] and *Argus and Heflin* [1995]) are significantly different from observed fault-normal and fault-parallel velocities [*Beavan et al.*, 1999].

[23] The predicted relative motion using our model is 39.5 ± 0.6 mm/yr fault-parallel and 8.5 ± 0.2 mm/yr fault-normal (computed at 43.5°S, 170°E assuming a fault strike of 56°). These values are essentially the same as those of *Tregoning et al.* [1998a] therefore there is still a misfit in fault-normal component between observed convergence across the fault and that predicted from plate models based on far-field GPS velocities, implying that the relative angular velocity vector for the Australian/Pacific Plate is not modeling well the relative motion between the two plates on either side of the Alpine Fault in New Zealand. This can only occur if the model for either the Australian or Pacific Plate is not correct.

[24] Our model for the motion of the Australian Plate fits the observed GPS velocities very closely. Rates of change of baseline lengths between these sites are typically <1 mm/yr, and none are significantly different from zero at the 1σ level. The model for the Pacific Plate does not fit the observed GPS velocities to the same level; therefore any errors in our derived relative angular velocity vector for these two plates probably arises from errors in the angular velocity vector for the Pacific Plate itself. In particular, the velocity at CHAT with respect to the Pacific Plate is almost significantly different from zero, a result also found by *DeMets and Dixon* [1999]. Perhaps the entire Pacific Plate is not moving as

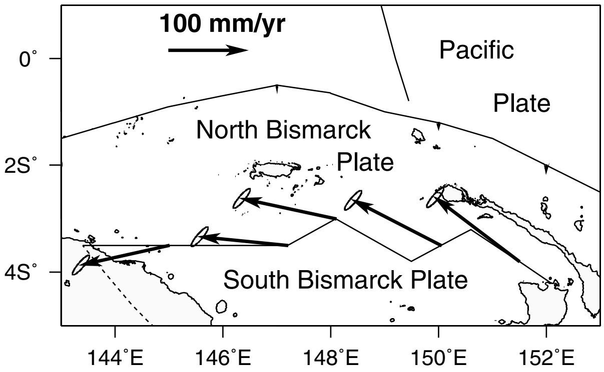

Figure 6. Predicted motions of the North Bismarck Plate relative to the South Bismarck Plate along the Bismarck Sea Seismic Lineation.

a totally rigid body and one should model the northern and southern regions of the plate separately.

[25] We do not have sufficient distribution of GPS sites in the southern region to allow us to solve for an angular velocity vector based on only southern hemisphere sites. However, the predicted motions using the angular velocity vector for the Pacific Plate derived using only sites in the Northern Hemisphere (that is, excluding CHAT) (64.7°S, 114.4°E, 0.647°/Myr) fits the velocities at these sites more closely but misfits the velocity of CHAT by +2.4 mm/yr north, −0.3 mm/yr east. This may explain the discrepancy between global plate model predictions and local observations of convergence rate across the Alpine Fault.

[26] The results of this study initiated an in-depth analysis of the motion of the Pacific Plate using 11 sites distributed across the Pacific Plate (J. Beavan et al., "The motion and rigidity of the Pacific Plate", submitted to *Journal of Geophysical Research*, 2000). While there is little supporting geophysical/geological evidence for there being separate North and South Pacific Plates, there does appear to be coherent geodetic evidence that the New Zealand continental shelf is moving relative to the Pacific Plate.

5.2. North Bismarck/Pacific Boundary

[27] The Pacific and North Bismarck Plates share a boundary along the Manus Trench (assuming that there is no Caroline Plate) and possibly the Kilinailau Trench to the east of New Ireland. There is very little seismicity along these trenches which has led some authors [e.g., *Curtis*, 1973; *Krause*, 1973] to speculate that they are no longer active subduction zones. *Johnson and Molnar* [1972] predicted that relative motion of 10 mm/yr with an azimuth of 114° occurred between these two plates. Assuming that these trenches form the boundary between these two plates and that all convergence is accommodated there, our relative angular velocity vector for the two plates predicts relative motion on the Manus Trench of 7.6 ± 0.1 mm/yr with an azimuth of 172.4 ± 0.4° (1.2°S, 148°E) and on the Kilinailau Trench of 10.3 ± 0.1 mm/yr with an azimuth of 177.8 ± 0.2° (2.2°S, 152.3°E). The relative motion on the Manus Trench is roughly normal to the trench, while the relative motion across the Kilinailau Trench implies a convergent component of ~9.4 ± 0.8 mm/yr and a right-lateral along-strike component of ~4.2 ± 0.2 mm/yr, assuming that the trench strikes 112° (Figure 5).

5.3. North Bismarck/South Bismarck Boundary

[28] The North and South Bismarck Plates interact along the Bismarck Sea Seismic Lineation (BSSL). *Taylor* [1979] described this boundary as a "leaky" transform fault in the west, a NE-SW trending ridge and scarp, a section of spreading zone farther east and another strike-slip region running NW-SE near New Ireland (Figure 6). *Martinez and Taylor* [1996] described a microplate, the Manus Plate, located between the North and South Bismarck Plates on the southern side of the Manus Spreading Center.

[29] The relative motion predicted by this study along this boundary is shown in Figure 6. The motion is predominantly strike-slip along the western end of the BSSL, although there is a convergent component in the far west which becomes divergent east of 146.5°E. Spreading of ~129 ± 6 mm/yr is predicted on the spreading center, although the Manus Microplate is probably interacting with the North Bismarck Plate here. The predicted motion of 137 ± 5 mm/yr at the eastern end of the BSSL is parallel to the known transform faults in the region.

[30] The location of the boundary between the North and South Bismarck Plates across New Ireland is not known although *Tregoning et al.* [2000] identified a broad deformation zone from GPS velocities spanning New Britain and southern New Ireland. It is possible that the transition from the South Bismarck Plate to the Pacific Plate (through the North Bismarck Plate) is widely distributed and occurs over a broad zone. Work is continuing to better understand the interaction of the three plates in the region.

6. Conclusions

[31] Improved temporal and spatial distribution of GPS data has led to significant improvements in the geodetic estimates of site velocities in the Australasian and Pacific regions. In particular, the densification of the IGS network and the vast amounts of data which are now freely available allow large-scale regional analyses to be made. We used these data, augmented with data collected in several campaigns in Papua New Guinea and Indonesia, to revise the estimates of the angular velocity vectors which can be used to predict motion of the Australian, Pacific, and North Bismarck Plates. The angular velocity vectors presented here fit the available geodetic data and represent a significant improvement in the accuracy of modeling plate motions in the western Pacific. These angular velocity vectors can be used in conjunction with geodetic velocity fields near plate boundaries to remove the rigid plate motion and produce accurate relative velocity fields at the plate boundaries.

[32] The revision of the Pacific Plate angular velocity vector has allowed discrepancies in motion relative to the Pacific Plate to be detected at sites located north of the Bismarck Sea Seismic Lineation. This provides strong evidence for the existence of a North Bismarck Plate, and we estimated the angular velocity vector for this plate from three GPS site velocities. The relative angular velocity vector between the North Bismarck and Pacific Plates predicts convergence on the Manus Trench of ~9 ± 0.5 mm/yr, while relative motion along the Kilinailau Trench is ~10 ± 0.3 mm/yr and is oblique to the strike of the trench.

Appendix A: Geodetic Analysis

[33] The analysis procedures used here are described in detail, for example, by *Feigl et al.* [1993], *Dong et al.* [1998], *Tregoning et al.* [1998a]. In this appendix we provide information to demonstrate that the methodology has been applied carefully and that the geodetic solution is robust and correctly attached to the ITRF.

[34] The data used in the analysis comprise daily solutions of GPS phase measurements from a global polyhedron of GPS tracking sites. The number of sites varies from ~30 in 1991 to over 80 in 2000. Prior to 1995, all data were combined in a single daily solution. After 1995 the global tracking data were divided into three subnetworks (approximately the three regions of (1) the Southern Hemisphere, (2) the Asia-Pacific region, and (3) Europe/North America) with at least four common sites between subnetworks. These subnetwork solutions were then combined to produce a single daily estimate of the satellite orbits and the coordinates of a global polyhedron of sites. It can be shown that the combination yields the same result as processing all the data simultaneously but

the former approach takes significantly less processing time. In all cases the data collected in campaign-style observations at sites in Papua New Guinea and Indonesia were included in the global analysis. Our satellite orbits agree with the IGS orbits at the ~7–8 cm level root-mean-square. In fact, using the same processing methodology *Tregoning et al.* [1998b] showed considerable improvement in orbit estimates over the IGS orbits for data in late 1995.

[35] We then combined the daily solutions to form a ''fiducial-free'' network, with parameters of site coordinates and velocities. During this combination we may model the errors in site coordinates and velocities as any combination of white noise or red noise by allowing stochastic variation of the parameters. We applied 0.33 mm^2/yr stochastic noise to account for the red noise characteristics seen in GPS time series [*Johnson and Agnew*, 2000].

[36] Owing to the immense amount of data observed since 1993, we have not yet computed daily solutions for every day. Instead, global solutions have been computed when data have been collected at specific sites of interest. The data used comprise campaign-style data in 1991–1994 (typically ~10 days/yr) and significantly more in subsequent years (1995, 90 days; 1996, 70 days; 1997, 100 days; 1998, 160 days; 1999, 50 days; 2000, 70 days). We tested the robustness of the solution by computing a velocity field using only 7 days data in each year of 1995–2000. The changes in the velocity estimates were <2 mm/yr, indicating that continuous daily estimates are not required in order to estimate velocities with an accuracy of ~2 mm/yr providing the time span of the data is sufficiently long.

[37] One could have chosen to process only the regional data and then to combine the solutions with global solutions available from IGS Analysis Centers or, alternatively, to fix IGS orbits, satellite clocks, and Earth orientation parameters and to solve for site coordinates using single-point positioning methods [*Zumberge et al.*, 1997]. We chose to compute our own global solutions because it afforded us the flexibility to define the terrestrial reference frame at the last stage of the processing procedure and to be able to change the definition without having to reprocess all the data. Furthermore, we can be sure that all our solutions are based on a consistent methodology (e.g., satellite orbital force model, site elevation cutoff angles, etc.).

[38] We computed seven-parameter Helmert transformations of the coordinates and velocities of the 47 class A and B IGS core GPS sites [*Altamimi*, 1998] to align our ''fiducial-free'' network with the ITRF97 (in fact, a six-parameter transformation suffices (three rotations, three translations) because the scale factor difference between our network and ITRF97 is not significant). The root-mean-square of the position and velocity transformations were 3.9 mm and 0.6 mm/yr, respectively.

[39] Transforming our solution in this manner inherently implies that the resulting velocity field is then dependent on the coordinates and velocities of ITRF97. This is true, although it is less dependent than if one had ''fixed'' the coordinates and velocities to their ITRF97 values. Nonetheless, it would also be true if a smaller number of fiducial sites were used in the transformation, although the result would then be more dependent on each individual velocity because the degrees of freedom of the transformation would be reduced.

[40] In order to test the strength of the influence of these 47 sites on the final velocity field, we computed transformations using only the original 13 core IGS sites [*Boucher et al.*, 1996]. The variation in the resulting velocity field was <2 mm/yr, typically <1 mm/yr at most sites. Thus the use of 47 fiducial sites to compute the Helmert transformations is not significantly biasing the estimated velocity field any more than using a subset of these sites.

[41] Some of the sites used in the transformations are located on the Australian (YAR1, PERT, TIDB, AUCK) and Pacific (KWJ1, KOKB, CHAT) Plates, the two major plates whose motions are defined in this paper. We recomputed the transformations using only core sites which were not on either of these two plates in order to check whether we were unfairly forcing the angular velocity vectors of these two plates. The changes in the velocities of sites on the Australian and Pacific Plates were <2 mm/yr when transforming our network into ITRF97 without using these sites, and the effect on the angular velocity vector estimates was <1° in position and negligible in rotation rate.

[42] **Acknowledgments.** I thank staff at the Papua New Guinea National Mapping Bureau and staff and students at the Papua New Guinea University of Technology, Lae, for their assistance in conducting fieldwork in 1993, 1996, 1998, and 2000 to collect the GPS data used in this analysis. I thank T. Kato for providing GPS data from the TRUK site. I also thank the IGS and AUSLIG for making available global and regional tracking data used in this analysis, H. McQueen for fruitful discussions, and W. Simons, K. Larson, and B. Parsons for helpful review comments. Figures were plotted using the GMT software [*Wessel and Smith*, 1991].

References

Altamimi, Z., IGS reference stations classification based on ITRF96 residual analysis, paper presented at the IGS Workshop, Int. GPS Serv., Darmstadt, Germany, 9–11 Feb. 1998.

Argus, D. F., and R. G. Gordon, No-net-rotation model of current plate velocities incorporating plate motion model NUVEL-1, *Geophys. Res. Lett.*, *18*, 2039–2042, 1991.

Argus, D. F., and M. B. Heflin, Plate motion and crustal deformation estimated with geodetic data from the Global Positioning System, *Geophys. Res. Lett.*, *22*, 1973–1976, 1995.

Beavan, J., et al., Crustal deformation during 1994-1998 due to oblique continental collision in the central Southern Alps, New Zealand, and implications for seismic potential of the Alpine Fault, *J. Geophys. Res.*, *104*, 25,233–25,255, 1999.

Boucher, C., Z. Altamimi, M. Feissel, and P. Sillard, Results and analysis of the ITRF94, (ITRF94), *Tech. Note 20*, Int. Earth Rotation Serv., Obs. de Paris, Paris, 1996.

Boucher, C., Z. Altamimi, and P. Sillard, The ITRF97 International Terrestrial Reference Frame (ITRF97), *Tech. Note 27*, Int. Earth Rotation Serv., Obs. de Paris, Paris, 1999.

Curtis, J. W., Plate tectonics of the Papua New Guinea–Solomon Islands region, *J. Geol. Soc. Aust.*, *20*, 1–19, 1973.

DeMets, C., and T. H. Dixon, New kinematic models for Pacific–North America motion from 3 Ma to present, I, Evidence for steady motion and biases in the NUVEL-1A model, *Geophys. Res. Lett.*, *26*, 1921–1924, 1999.

DeMets, C., R. G. Gordon, D. F. Argus, and S. Stein, Current plate motions, *Geophys. J. Int.*, *101*, 425–478, 1990.

DeMets, C., R. G. Gordon, D. F. Argus, and S. Stein, Effect of recent revisions to the geomagnetic reversal time scale on estimates of current plate motions, *Geophys. Res. Lett.*, *21*, 2191–2194, 1994.

Dong, D., T. A. Herring, and R. W. King, Estimating regional deformation from a combination of space and terrestrial geodetic data, *J. Geod.*, *72*, 200–214, 1998.

Feigl, K., et al., Space geodetic measurements of crustal deformation in central and southern California, 1984–1992, *J. Geophys. Res.*, *98*, 21,677–21,712, 1993.

Herring, T. A., GLOBK global Kalman filter VLBI and GPS analysis program, version 4.1, Mass. Inst. of Technol., Cambridge, 1999.

Johnson, H. O., and D. C. Agnew, Correlated noise in geodetic time series, June 1, 1997–May 31, 1999, final technical report to USGS, Inst. of Geophys. and Planet. Phys., Univ. of Calif., San Diego, 2000.

Johnson, R. W., and P. Molnar, Focal mechanisms and plate tectonics of the southwest Pacific, *J. Geophys. Res.*, *77*, 5000–5032, 1972.

Kato, T., Y. Kotake, T. Chacin, Y. Iimura, S. Miyazaki, T. Kanazawa, and K. Suyehiro, An estimate of the Philippine Sea Plate motion derived from the global positioning system: Observations at Okino Torishima, *J. Geod. Soc. Jpn.*, *42*, 223–243, 1996.

Kato, T., et al., Initial results from WING, the continuous GPS network in the western Pacific area, *Geophys. Res. Lett.*, *25*, 369–372, 1998.

King, R. W., and Y. Bock, Documentation for the GAMIT GPS anaylsis software, release 9.6, Mass. Inst. of Technol., Cambridge, 1999.

Kotake, Y., T. Kato, S. Miyazaki, and A. Sengoku, Relative motion of the Philippine Sea Plate derived from GPS observations and tectonics of the south-western Japan, *J. Seismol. Soc. Jpn.*, *51*, 171–180, 1998.

Krause, D. C., Crustal plates of the Bismarck and Solomon Seas, in *Ocea-*

nography of the South Pacific 1972, edited by R. Frazer, pp. 271–280, N. Z. Natl. Comm. for UNESCO, Wellington, 1973.
Larson, K., J. T. Freymueller, and S. Philipsen, Global plate velocities from the Global Positioning System, *J. Geophys. Res.*, *102*, 9961–9981, 1997.
Manning, J., R. Govind, and P. Holland, The monitoring of national and regional geodetic networks, paper presented at International Workshop on Advances in Deformation Monitoring, Curtin Univ. of Technol., Perth, Western Australia, 24–25 Sept. 1998.
Mao, A., C. G. A. Harrison, and T. H. Dixon, Noise in GPS coordinate time series, *J. Geophys. Res.*, *104*, 2797–2816, 1999.
Martinez, F., and B. Taylor, Backarc spreading, rifting and microplate rotation, between transform faults in the Manus Basin, *Mar. Geophys. Res.*, *18*, 203–224, 1996.
McClusky, S. C., K. Mobbs, A. Stolz, D. Barsby, W. Loratung, K. Lambeck, and P. Morgan, The Papua New Guinea satellite crustal motion surveys, *Aust. Surv.*, *39*, 194–214, 1994.
Seno, T., S. Stein, and A. E. Gripp, A model for the motion of the Philippine Sea Plate consistent with NUVEL-1 and geologic data, *J. Geophys. Res.*, *98*, 17,941–17,948, 1993.
Sillard, P., Z. Altamimi, and C. Boucher, The ITRF96 realization and its associated velocity field, *Geophys. Res. Lett.*, *25*, 3223–3226, 1998.
Taylor, B., The Bismarck Sea: Evolution of a back-arc basin, *Geology*, *7*, 171–174, 1979.
Tregoning, P., F. K. Brunner, Y. Bock, S. S. O. Puntodewo, R. McCaffrey, J. F. Genrich, E. Calais, J. Rais, and C. Subarya, First geodetic measurement of convergence across the Java Trench, *Geophys. Res. Lett.*, *21*, 2135–2138, 1994.
Tregoning, P., et al., Estimation of current plate motions in Papua New Guinea from Global Positioning System observations, *J. Geophys. Res.*, *103*, 12,181–12,203, 1998a.
Tregoning, P., R. Boers, D. M. O'Brien, and M. Hendy, Accuracy of precipitable water vapour estimation from GPS observations, *J. Geophys. Res.*, *103*, 28,901–28,910, 1998b.
Tregoning, P., R. J. Jackson, H. McQueen, K. Lambeck, C. Stevens, R. P. Little, R. Curley, and R. Rosa, Motion of the South Bismarck Plate, Papua New Guinea, *Geophys. Res. Lett.*, *26*, 3517–3520, 1999.
Tregoning, P., H. McQueen, K. Lambeck, R. Jackson, R. Little, S. Saunders, and R. Rosa, Present-day crustal motion in Papua New Guinea, *Earth Planets Space*, *52*, 727–730, 2000.
Weiler, P. D., and R. S. Coe, Rotations in the actively colliding Finisterre Arc Terrane: Paleomagnetic constraints on Plio-Pleistocene evolution of the South Bismarck microplate, northeastern Papua New Guinea, *Tectonophysics*, *316*, 297–325, 2000.
Weissel, J. K., and R. N. Anderson, Is there a Caroline plate?, *Earth Planet. Sci. Lett.*, *41*, 143–158, 1978.
Wessel, P., and W. H. F. Smith, Free software helps map and display data, *Eos Trans. AGU*, *72*, 441, 445–446, 1991.
Zumberge, J. F., M. B. Heflin, D. C. Jefferson, M. M. Watkins, and F. H. Webb, Precise point positioning for the efficient and robust analysis of GPS data from large networks, *J. Geophys. Res.*, *102*, 5005–5017, 1997.

P. Tregoning, Research School of Earth Sciences, Australian National University, Canberra, A.C.T., 0200, Australia. (pault@rses.anu.edu.au)